

# A Study of Prompt Fast Ion Losses From Neutral Beam Injection in the DIII-D Tokamak

By Derek A. Sutherland

Submitted to the Department of Nuclear Science and Engineering in Partial Fulfillment of the Requirements for the Degree of

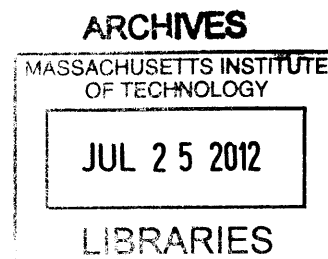
**Bachelor of Science in Nuclear Science and Engineering**

at the

**Massachusetts Institute of Technology**

June 2012

Derek A. Sutherland. All Rights Reserved.



The author hereby grants to MIT permission to reproduce and to distribute publicly paper and electronic copies of this thesis document in whole or part.

Work supported by U.S. DOE under the National Undergraduate Fusion Fellowship: DE-FC02-04ER54698,

DE-AC04-06OR23100, and SC-G903402.

Signature of Author: \_\_\_\_\_

Department of Nuclear Science and Engineering

May 11, 2012

Certified By: \_\_\_\_\_

Dennis Whyte

Professor of Nuclear Science and Engineering

Thesis Supervisor & Reader

Accepted By: \_\_\_\_\_

Dennis Whyte

Professor of Nuclear Science and Engineering

Chairman, NSE Committee for Undergraduate Students

# **A Study of Prompt Fast Ion Losses From Neutral Beam Injection in the DIII-D Tokamak**

By

**Derek A. Sutherland**

Submitted to the Department of Nuclear Science and Engineering on May 11, 2012

In Partial Fulfillment of the Requirements for the Degree of

Bachelor of Science in Nuclear Science and Engineering

## **ABSTRACT**

A study of the prompt losses of injected neutral beam born fast ions was conducted on the DIII-D tokamak at General Atomics using scintillator based fast ion loss detectors (FILD) and a reverse orbit calculation code. Prompt losses, also called first orbit losses, result from injected neutrals that are ionized on orbits that terminate to the outer wall before making a complete neoclassical, poloidal revolution. A strike map code has been developed which generates meshes that overlay optical fast ion signals from the FILD scintillator, providing a measurement of the pitch angles and gyroradii of incident fast ions. The pitch angles and gyroradii of incident ions are inputs to a reverse orbit calculation code used to calculate the trajectories of the incident ions in reverse time back to their birth at the intersection of the reverse orbit and an overlaid neutral beam injection footprint. The megahertz (MHz) sampling frequency of the FILD scintillator, along with finer time resolution neutral beam signals, enabled a comparison of the measured time delay between the onset of the neutral beam injection and the measured FILD loss signals with the calculated transit time based on the path length of the simulated reverse orbit. Consistency between the experimentally measured transit times and the simulation orbit times was observed. This result indicates the generated strike maps which provide a measurement of incident ions' gyroradii and pitch angles are accurate. This study supplements current studies seeking to improve the understanding of fast ion transport due to magnetohydrodynamic (MHD) activity, such as reverse shear Alfvén eigenmodes (RSAEs) and toroidal Alfvén eigenmodes (TAEs), which will be of great importance for predominately self-heated reactor scenarios.

Thesis Supervisor: Dennis Whyte

Title: Professor of Nuclear Science and Engineering

## Contents

<b>Introduction</b>	<b>5</b>
Controlled Fusion Energy . . . . .	5
Power Balance . . . . .	7
Neutral Beam Injection and Prompt Losses . . . . .	8
<b>Diagnostics and Computational Tools</b>	<b>10</b>
Fast Ion Deuterium-Alpha (FIDA) Diagnostic . . . . .	11
Fast-Ion Loss Detector (FILD) . . . . .	12
Application of Diagnostics . . . . .	16
Reverse-Orbit Calculation Code . . . . .	17
<b>Objective</b>	<b>19</b>
<b>Methodology</b>	<b>20</b>
<b>Results</b>	<b>22</b>
Summary . . . . .	22
FILD1 Results . . . . .	23
FILD2 Results . . . . .	24
<b>Discussion and Conclusion</b>	<b>26</b>

**Extensions**

**28**

**References**

**29**

# Introduction

## Controlled Fusion Energy

Over the past sixty years, the prospect of controlled magnetic fusion energy has been pursued through various experimental methods, all motivated by the benefits of a nearly unlimited fuel supply, zero greenhouse emissions, and limited short-lived radioactive byproducts. The necessity of any fusion reactor is that the total energy released from fusion reactions must both be capable of maintaining thermonuclear temperatures and can be transformed into electricity. Though a net gain fusion reactor has been elusive thus far, there have been many advances made in past decades primarily on the most researched fusion concept, the tokamak, which suggest a tokamak fusion reactor may be physically tractable. Even so, magnetic fusion energy must still be demonstrated as a tractable energy source via a burning plasma experiment, one in which fusion born charged particles are the predominate sources of energy to maintain thermonuclear temperatures. One such experiment named ITER is presently under construction in France, and will be the first controlled thermonuclear fusion experiment that produces more energy than is required as input.

The fusion reaction to be used in ITER and other first generation fusion reactors is the deuterium-tritium (DT) reaction, a decision motivated by the relatively high cross section of this fusion reaction when compared to other common reactions, as depicted in Figure 1.[6] The DT fusion reaction yields an energetic alpha particle and neutron with 3.5 MeV and 14.1 MeV of kinetic energy, respectively. Since the alpha particle is charged, it executes gyromotion due to the presence of magnetic fields, and deposits its energy through coulomb collisions with plasma species as it comes into thermal equilibrium with the relatively cooler, ambient plasma. Thus, if alpha particles are present in a sufficient amount and are confined for a long enough time to allow thermalization to occur within the background plasma, they can maintain the thermonuclear temperatures required to perpetuate fusion reactions. The neutron, which carries 80% of energy yield from a DT fusion reaction due to momentum

considerations, is uncharged and thus leaves the fusion system. The neutron is moderated in a blanket structure, producing heat that will be transformed into electricity through typical heat engine methods. Thus, due to the ease of the DT fusion reaction coupled with its favorable products to both maintain a burning plasma and provide a source of energy for electricity production using conventional heat engine technology, this is the type of fusion to be implemented in ITER and other first generation fusion reactors.

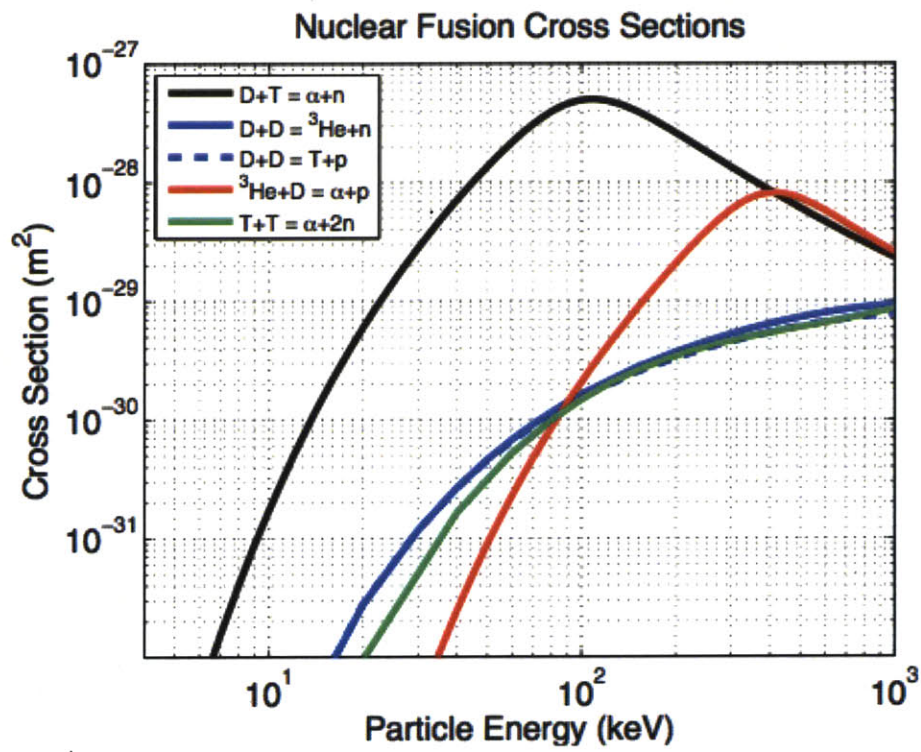


Figure 1. Fusion reaction cross sections versus energy. Note the substantially higher probability of DT fusion events when compared to other fusion reactions in the experimentally practical temperature range of 10 to 40 keV.[6]

## Power Balance

Studies of fast-ion losses in fusion systems are of current importance as a move towards predominately self-heated fusion experiments is imminent. ITER, which is presently under construction, is a large scale, tokamak fusion experiment where the alpha particles, the charged product from the deuterium-tritium (DT) fusion reaction, will become the dominate source of energy in the power balance of the system,[4]

$$S_{\alpha} + S_h = L_b + L_E \quad (1)$$

where  $S_{\alpha}$  and  $S_h$  are the sources of energy from alpha particles and external heating, respectively.  $L_b$  is the loss of power from the system due to bremsstrahlung, the inevitable electromagnetic radiation that is emitted when electrons undergo accelerations during coulomb collisions, and  $L_E$  is rate of energy loss through conduction from a hot material, the thermonuclear plasma, to the cooler environment, the first material wall, characterized by the energy confinement time  $\tau_E$ . Rewriting this formula in terms of commonly used plasma conditions of pressure  $p$ , temperature  $T$ , energy confinement time  $\tau_E$  and the other known quantities of volume averaged fusion reaction rate  $\langle \sigma \nu \rangle$ , alpha particle energy  $E_{\alpha}$ , bremsstrahlung constant  $C_b$  and externally applied heating power  $S_h$ , [4]

$$\left(\frac{E_{\alpha}}{16}\right) \frac{p^2 \langle \sigma \nu \rangle}{T^2} + S_h = \frac{C_b}{4} \frac{p^2}{T^{3/2}} + \frac{3}{2} \frac{p}{\tau_E} \quad (2)$$

In a predominately self-heated DT fusion reactor, commonly known as a burning plasma, the main source of energy in the system will be the alpha power,  $S_{\alpha}$ , with only a small portion of additional heating power required to achieve power balance and maintain some external control of plasma current profiles. A loss of energetic alpha particles from a burning plasma before thermalization can occur could jeopardize fusion power balance and lead to a plasma quench if additional heating power cannot be immediately injected to compensate for

this unexpected, large loss of alpha particle power. Also, energetic alpha particles ejected from the fusion system before thermalizing could damage first wall components that are inundated with these energetic charged particles. Large scale ejections of alpha particles from a self-heated fusion system can result from unmitigated magnetohydrodynamic (MHD) instabilities, such as reversed shear and toroidal Alfvén eigenmodes.[2,10] Since 3.5 MeV alpha particles are supersonic relative to typical Alfvén speeds in a fusion system, their shockwaves can induce Alfvén eigenmodes which can subsequently enhance fast ion transport. Thus, fast-ion loss mechanisms such as fast ion induced MHD instabilities and the subsequent degradation of fast ion confinement must be well understood and properly mitigated to ensure the success of self-heated fusion reactors such as ITER and future electricity producing fusion reactors.

### **Neutral Beam Injection and Prompt Losses**

Since most present experiments run solely on deuterium, the fusion born fast ion population is quite low due to the small reaction rate for deuterium-deuterium (DD) fusion relative to DT fusion rates at usual operating temperatures of a few kilo-electron-volts (keV), depicted in Figure 1.[6] Even without sufficient energetic ions from fusion events in present experiments, one can study energetic ion transport using neutral beam systems, which inject energetic neutral deuterium atoms of different molecular configurations into the fusion plasma. These neutrals are unaffected by the magnetic fields present while the machine is operating, which enables penetration into the plasma rather than being diverted to the wall immediately upon entering the vacuum vessel. The neutrals are produced by a resonant charge exchange interaction while passing through a gas of deuterium, after they are electrostatically accelerated while they were ions. These neutrals are eventually re-ionized in the tokamak after coulombically colliding with the charged species comprising the fusion plasma. These energetic ions then thermalize with the background plasma after subsequent coulomb collisions, identically to how charged fusion products would reach thermal equilibrium in a self-heated



fusion system. Thus, neutral beams heat the plasma by injecting energetic neutrals that are ionized and then thermalized with the background plasma. This process is the foundation for research of neutral beam current drive (NBCD) for non-inductive, steady-state, tokamak operation scenarios.

The DIII-D tokamak at General Atomics has four neutral beam injectors stationed at multiple points around the torus, depicted in Figure 2 with other diagnostics that will be discussed.[10] The 210° neutral beam injects counter the conventional plasma current direction, and the 150° neutral beam injector can be vertically tilted to inject off-axis, up to 16° above the mid-plane of the torus. The four different neutral beam locations, with off-axis and counter plasma current injection capabilities, provide flexibility in the type of experiments that can be conducted on DIII-D. Fundamentally, these energetic neutral beam ions are governed by the Lorentz force law once ionized, which yields the force on a charged particle due to the direction and strength of the magnetic field where the charged particle is located at a particular time.

However, the energetic ions resulting from neutral beam injection do not always thermalize with the background plasma, and some are always lost from the system to the wall of the machine on the time scale of 10s to 100s of microseconds, well before thermalization can occur. These types of losses are referred to as prompt losses, or first orbit losses, where first orbit refers to the first neoclassical orbit traversed by the ion from its point of origin. A neoclassical orbit, or commonly referred to as a banana orbit because of its shape, results from magnetic mirroring in the  $R^{-1}$  toroidal magnetic field inherent to any toroidally shaped machine with externally applied toroidal magnetic fields. A banana orbit is depicted in Figure 3 in a poloidal cross section of a toroidal device.[1] If particles do not have a sufficient velocity parallel to the local magnetic field to traverse a mirroring point and continue their circular, poloidal revolutions, they become trapped in a magnetic mirror and undergo a banana shaped poloidal trajectory. First orbit losses are an inevitable loss of fast ions from the system while using neutral beam injection, and occur whenever the first

neoclassical orbit trajectory intersects the first wall of the tokamak. The radial excursion of the banana orbit increases with trapped particle energy, and thus is why fast ions are more prone to intersecting the wall when compared to thermalized ion species undergoing neoclassical orbits. These types of losses are able to be differentiated from other fast ion loss mechanisms such as MHD instabilities and microturbulence since they occur in phase with neutral beam injection, albeit with a small offset of 10s of microseconds that will be referred to throughout this paper as the transit time of a promptly lost fast ion. These transit times will be a key quantity of interest throughout this study.

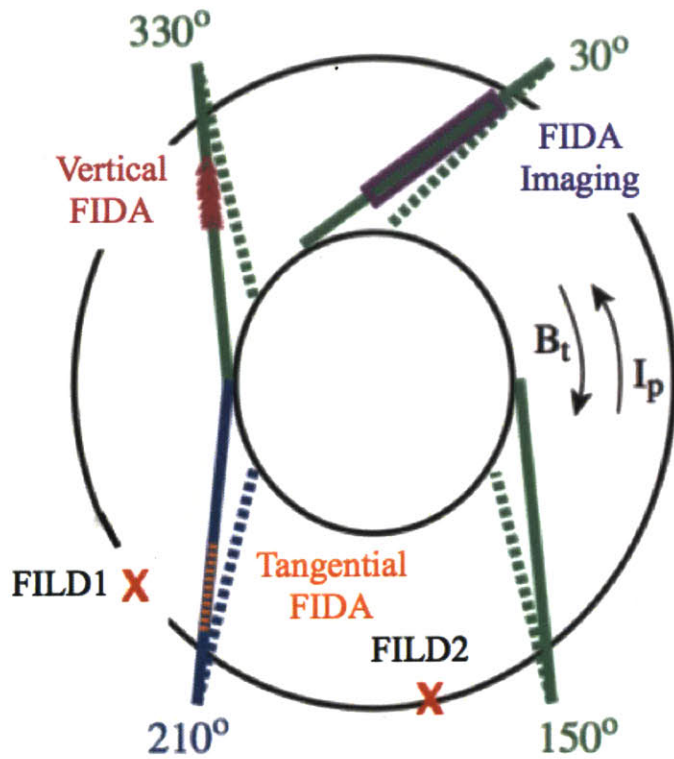


Figure 2. Top down view of the DIII-D tokamak showing neutral beam locations and both FIDA and FILD diagnostic system locations. Note the conventional directions of toroidal magnetic field  $B_t$  and plasma current  $I_p$  during operation, and that the 210° neutral beam injects in the counter plasma current direction.[10]

# Diagnostics and Computational Tools

## Fast Ion Deuterium-Alpha (FIDA) Diagnostic

The fast ion deuterium-alpha (FIDA) diagnostic system is used to study the fast ion distribution function in primarily externally heated devices such as DIII-D. As had been stated previously, a thorough understanding of fast ion transport for future, predominately self-heated fusion reactors is of utmost importance to ensure the success of these reactors. Any additional transport mechanisms amplified by a large population of energetic charged particles could jeopardize the power balance of a fusion system, and could also lead to serious damage to first wall components that are inundated with energetic charged particles. Using neutral beam injection or radio frequency heating, fast ion populations can be generated and allows the study of the confinement quality of energetic charged particles in currently operating deuterium devices.

The FIDA system provides a measurement of the  $D_\alpha$  spectrum resulting from a charge-

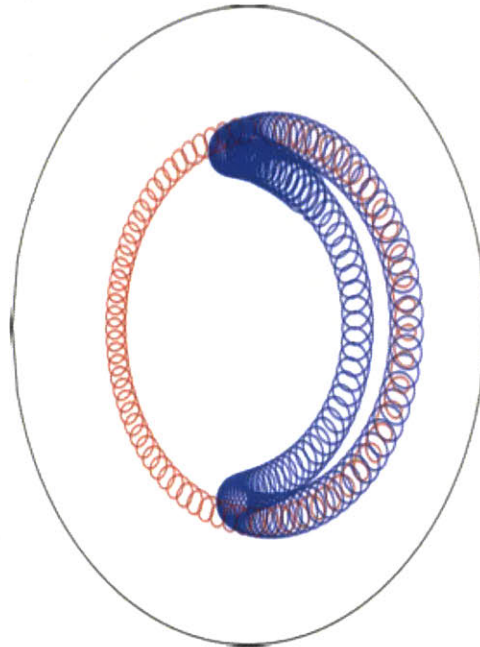


Figure 3. Poloidal orbits of a passing ion, the circular poloidal precession of a gyrating ion colored in red, and a trapped ion, the banana shaped poloidal precession of a gyrating ion colored in blue.[1]

exchange interaction between the neutral beam injected deuterium atoms and ambient plasma species, which yields doppler shifted light that reveals the presence of the energetic ions of interest in the plasma. There are a series of FIDA chords at varying spatial locations, mostly intersecting the neutral beam injection footprints where the charge-exchange interactions of interest are most likely to occur, as shown in Figure 4.[7] This spatial distribution of FIDA chords provides a measurement of the evolution of the fast ion distribution function. This FIDA system was used previously to indicate the onset of neutral beam injection into DIII-D, but neutral beam current signals that have finer time resolution than the FIDA signal are used in this study as a way to improve the precision of determining when fast ions begin executing gyromotion and undergoing neoclassical orbits once ionized in the fusion plasma.

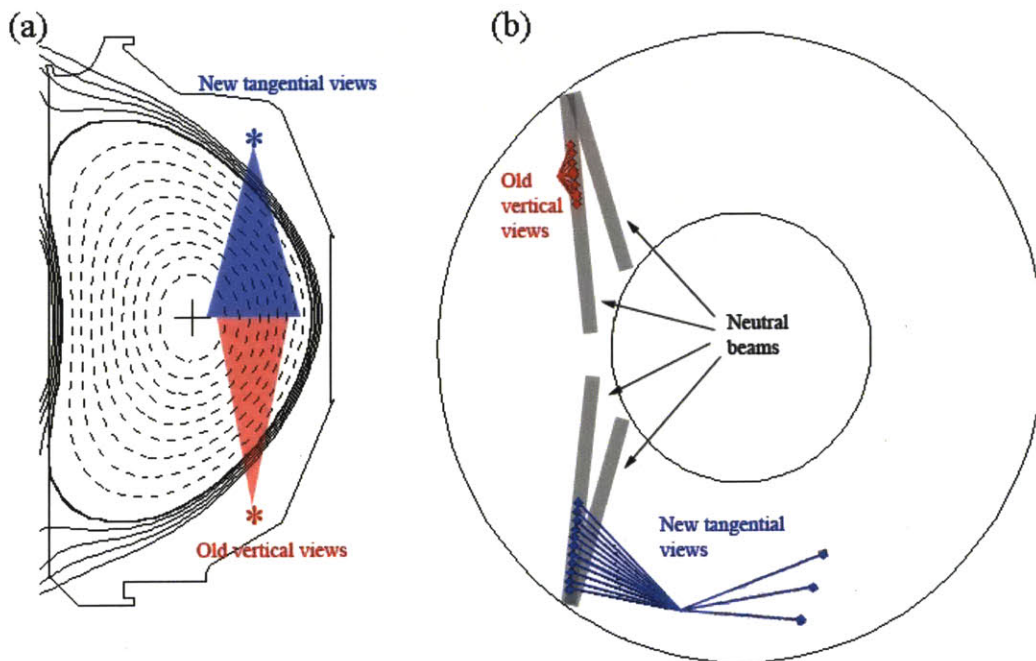


Figure 4. The poloidal and toroidal locations of the FIDA systems implemented on the DIII-D tokamak.[7]

### Fast-Ion Loss Detector (FILD)

A scintillation based, fast ion loss detector (FILD) system has been employed for this study, and is depicted in Figure 5.[3] This detector allows energetic ions to enter through an aperture

and strike a scintillator. The light emitted from the scintillator is split and fed into a CCD camera and a fiber-optically coupled PMT. This detector provides a measurement of an incident fast ion's gyroradius  $r_i$ ,

$$r_i = \frac{m_{ion}v_{ion}}{qB} = \frac{\sqrt{2E_{ion}m_{ion}}}{qB} \quad (3)$$

which provides a measurement of the ion's energy given knowledge of the local magnetic field strength, ion mass, and ion charge, as shown in Equation 3. The detector also provides measurement a of the pitch angle of an incident ion, the angle between the guiding center velocity of the incident ion and the local magnetic field direction at the FILD aperture. Figure 6 depicts how the use of an aperture and detector geometry allows a measurement of these two ion parameters. A bellows enables translational freedom to vary the proximity of the aperture to the last closed flux surface of the fusion plasma. The choice of fast response scintillation materials, coupled to a PMT that is digitized at a megahertz (MHz) yields microsecond resolution of the spatially integrated FILD scintillator signal.[3] Typical optical signals from the FILD detector are depicted in Figure 7, with an overlaid strike map that provides a measurement of an incident fast ion's gyroradius and pitch angle.[8] These strike maps are generated using a code that requires the inputs of the magnetic field strength and direction at the FILD aperture using magnetic equilibrium profiles at the time of fast ion detection, and the geometry of the particular FILD detector and scintillator. A depiction of how this strike map is generated is provided in Figure 8.[5] The code produces iso-contours of gyroradius and pitch angle that are superimposed on the optical CCD signal of interest, providing the gyroradius and pitch of detected fast ions.



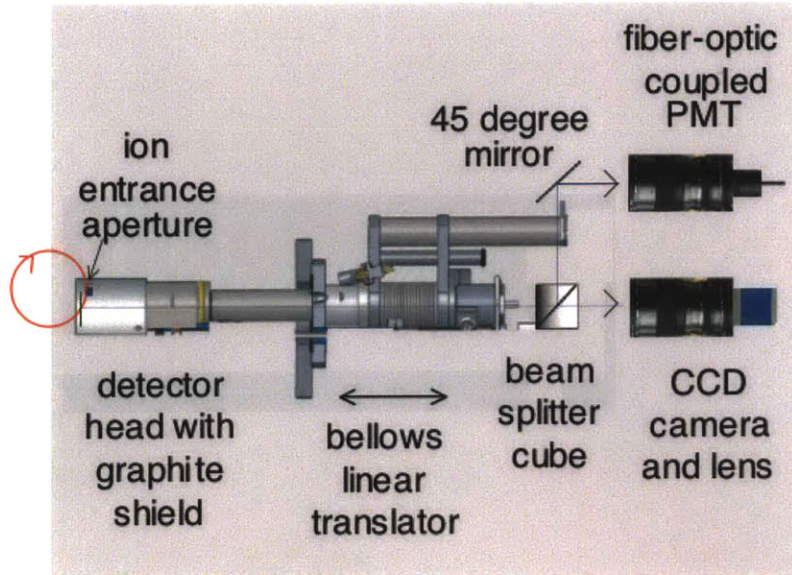


Figure 5. General schematic of the fast ion lost detectors (FILD) implemented on DIII-D.[3]

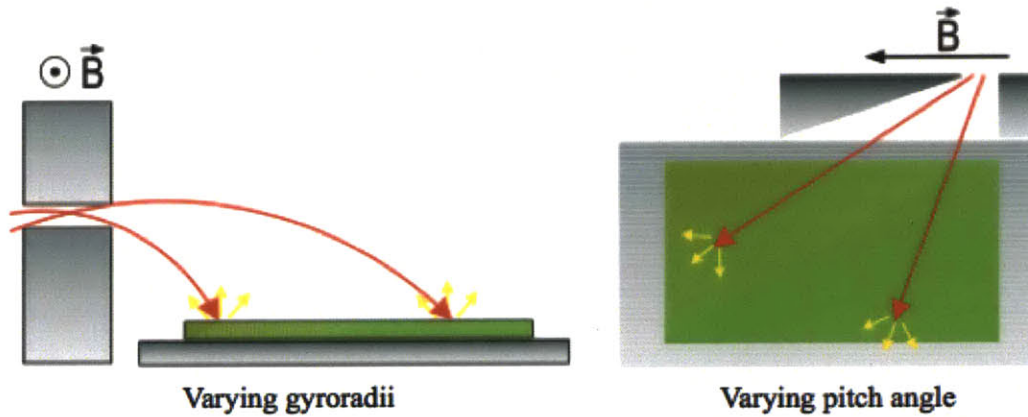


Figure 6. The geometry of the detector and aperture allow a measurement of an incident ion's gyroradius and pitch angle with respect to the local magnetic field direction.

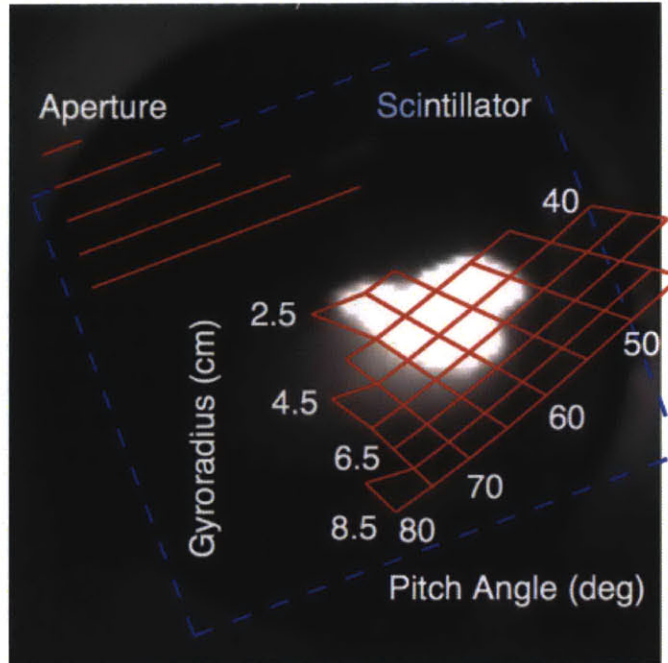


Figure 7. A typical FILD CCD camera signal with strike map overlaid. The observed ions have pitch angles varying from 50 to 65 degrees and gyroradii varying from 2.5 to 6.3 cm.[8]

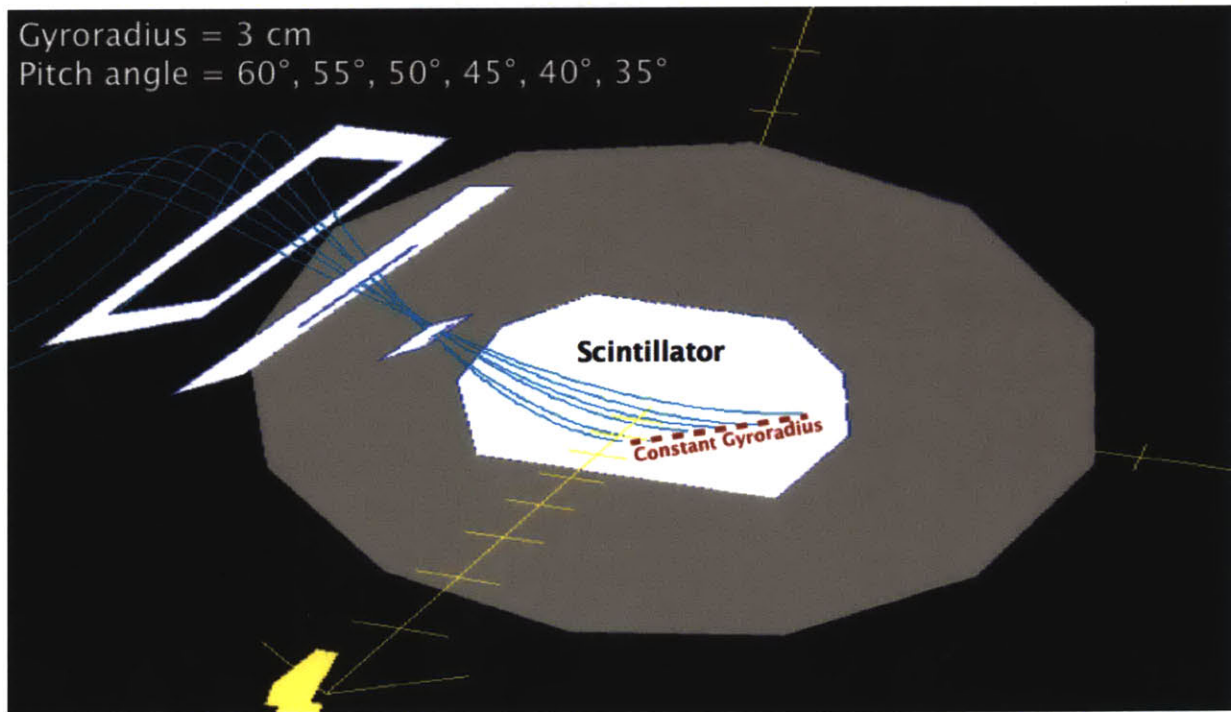


Figure 8. A simulation of the strike map calculation at fixed gyroradius and varying pitch angles. The scintillator is impacted with fast ions, and a series of apertures collimate the incoming fast ions. The strike map code then sweeps through various gyroradii (energies) of interest, and outputs a map to overlay an optical signal, and shown in Figure 7.[5]

## Application of Diagnostics

Neutral beam current signals are available on DIII-D which are digitized with ten microsecond time resolution. By measuring the time differential between the neutral beam current signals and FILD PMT signal, one can measure the transit time of a promptly lost fast ion from its birth to the FILD location where it was detected. Previously, the onset of neutral beams injection into the DIII-D tokamak was determined using the fast ion deuterium-alpha (FIDA) diagnostic near a toroidal location of a neutral beam of interest. However, the onset of the FIDA signal had a limited time resolution relative to the onset of the FILD PMT signal due to a relatively slow rise time of the FIDA signal, depicted in Figure 9.[3]

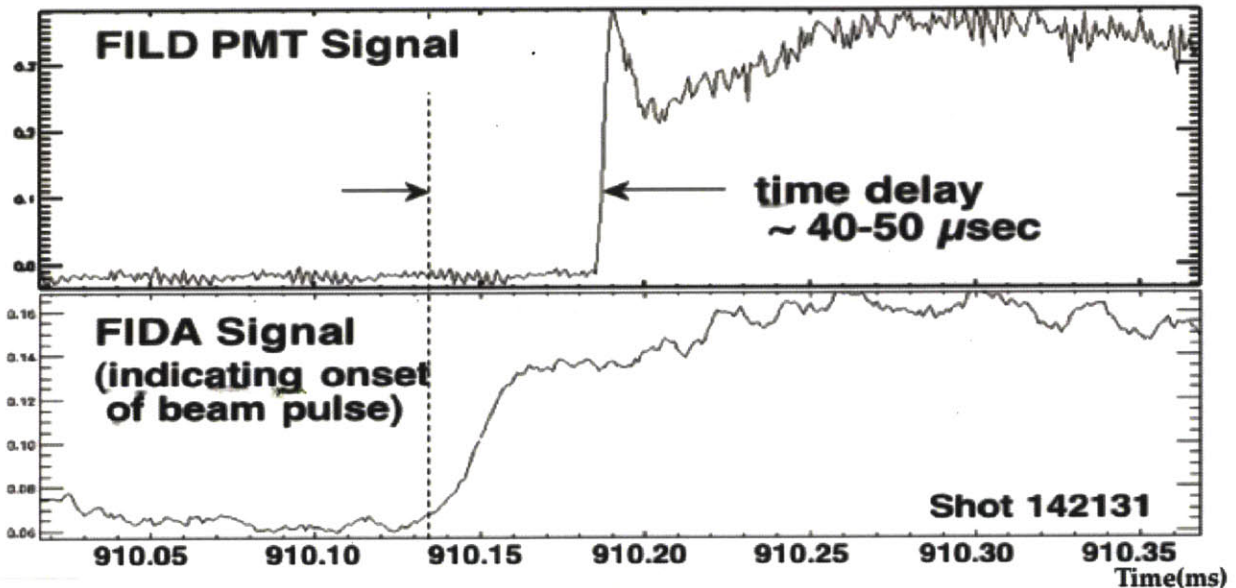


Figure 9. FIDA signal previously used to indicate the onset of neutral beam injection compared with the resulting FILD PMT signal. Note the relatively slow rise of the FIDA signal relative to the FILD PMT signal. The time delay indicated the approximate ion transit time from its birth to its intersection with the FILD scintillator.[3]

Despite time resolution still being limited by the neutral beam current being sampled every ten microseconds, the time resolution provided by these signals was substantially better than the FIDA signal, with roughly three times finer time resolution. An example of the neutral beam signal plotted with a resulting FILD signal is depicted in Figure 10, showing the noticeably shorter rise time of the neutral beam current signal above noise than the



FIDA signal while using similar time increments plotting. Using these two signals, transit times could be measured for particular sets of detected ions to better precision than had been previously possible, and were used substantially in this study. The DIII-D tokamak, with the neutral beam, FIDA diagnostics and FILD detector toroidal locations are depicted together in Figure 2 for the convenience of the reader.

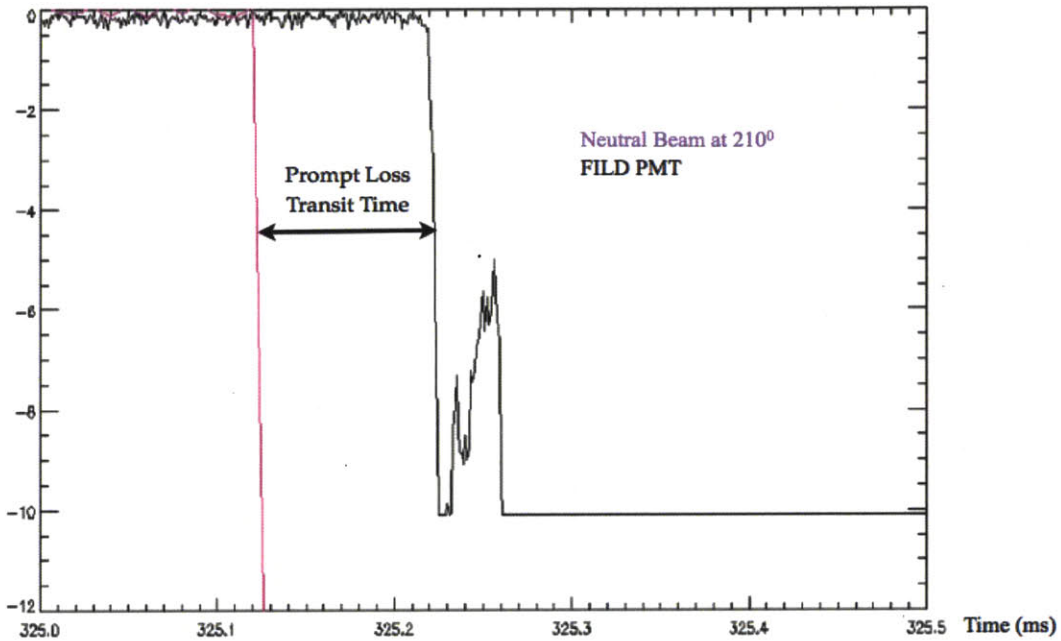


Figure 10. Neutral beam signals used in this study in place of the FIDA signals used previously, compared to the resulting FILD PMT signal. Negative values indicate the onset of neutral beam injection and FILD detection. The purple trace indicates the  $210^{\circ}$  neutral beam current turning on at 325.12 ms, and the black trace is the FILD PMT signal resulting from this neutral beam pulse upwards of 90 microseconds later. Note the substantially faster rise time of the purple neutral beam signal when compared to the FIDA signal depicted in Figure 9, which provided a more precise measure of the onset of neutral beam injection into DIII-D.

### Reverse-Orbit Calculation Code

The reverse-orbit calculation code used in this study calculates the full trajectory of fast ions incident on the FILD detector in reverse time to their likely points of origin. The code requires the inputs of the type of particle incident on the FILD detector, and the energy and pitch angles of incident particles. The code uses magnetic equilibrium profiles

and steps the particle trajectory back in time using the Lorentz force law, producing a fast ion trajectory in many different phase spaces, and provides the transit time for particular calculated trajectories. Using the feature to plot neutral beam footprints behind calculated ion trajectories and knowing which neutral beam produced particular observed fast ions, one can readily determine the range of possible transit times of detected fast ions. An example of a result used in this study from this reverse orbit calculation code is provided in Figure 11. This calculation is quite sensitive to the inputs of pitch angle and energies of detected ions, and thus fairly accurate strike maps that overlay the FILD scintillators to provide the required code inputs will be required to observe conformity between simulated and experimentally measured transit times.

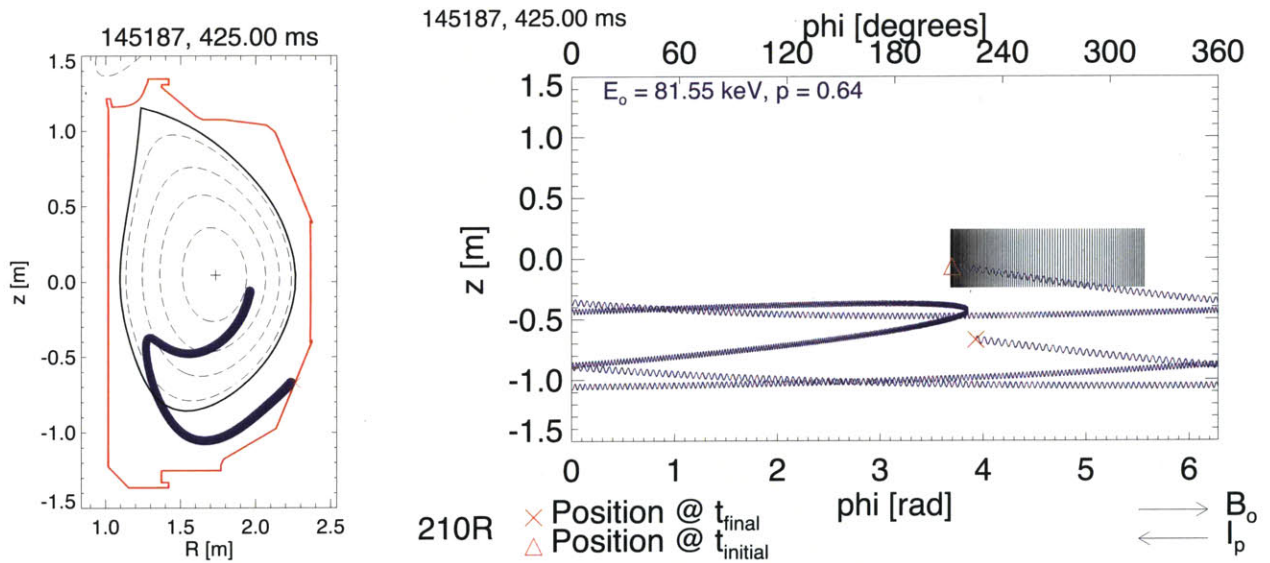


Figure 11. A typical result of the reverse orbit calculation code on a prompt loss measurement used in this study. The left plot provides the calculated reverse orbit in the poloidal plane, whereas the right plot depicts the reverse orbit in the toroidal plane. The initial and final locations on the right plot refer to a likely place of ionization and location of FILD detection, respectively. Note the banana orbit this fast ion was undergoing until it terminated at the FILD detector location near the first wall. Also, note that the initial fast ion velocity is counter the plasma current direction, which was expected since these losses result from the  $210^0$  neutral beam that injects countercurrently.

# Objective

The objective of this study was to validate the accuracy of generated strike maps that overlay FILD CCD signals, yielding a measurement on an incident ion's gyroradius and pitch angle. Previously, the fast-ion deuterium alpha (FIDA) imaging system was used as a temporal measurement of the onset of energetic neutrals undergoing charge-exchange interactions with ambient plasma species. The time resolution of the FIDA signal had previously limited the ability to determine the accuracy of generated FILD strike maps, primarily because of the relatively slow rise time of the FIDA system depicted in Figure 9.[3] This rise time was on the order of expected prompt-loss transit times, dozens of microseconds. By employing new neutral beam current signals with 10 microsecond time resolution, the transit times of promptly lost fast ions could be determined more accurately than was previously possible. With these more accurate prompt loss transit times, and using a methodology to be described in detail, the accuracy of the gyroradius and pitch angle strike maps could be more precisely determined. This study will also supplement other studies involving fast-ion transport by magnetohydrodynamic (MHD) activity such as reverse-shear Alfvén eigenmodes (RSAEs) and toroidal Alfvén eigenmodes (TAEs). The implications of fast-ion transport by Alfvén eigenmodes will also be discussed.

# Methodology

In order to validate the accuracy of generated strike maps, conformity between experimentally measured transit times of promptly lost fast ions and simulated transit times using a reverse orbit calculation code must be demonstrated. Neutral beam current signals and FILD PMT signals provide a measurement of the transit of fast ions that are injected as neutrals and are ionized at some point within the neutral beam spatial footprint. By observing the same pulsed, square waveform between the neutral beam current signal and FILD PMT offset by dozens of microseconds, one knows the FILD detector is measuring promptly lost fast ions resulting from neutral beam injection. By injecting only one neutral beam at a time, or by determining fast ions observed at a particular FILD detector location can only result from one neutral beam injector using the reverse orbit code neutral beam footprint feature, one can definitively determine which neutral beam is producing FILD detected, promptly lost fast ions. Thus, the repeated time differential between the neutral beam current signals and FILD PMT signals allows a repeated measurement of the transit time of promptly lost fast ions resulting from a particular neutral beam injector.

A reverse orbit calculation code has been employed to calculate the expected transit time of particles in reversed time from the point of detection to likely locations of origin. The code requires the inputs of the detected particle type, gyrophase, pitch angle, and particle energy. The latter two of these inputs are obtained using the generated meshes overlaying the FILD CCD camera signal at a particular time of interest, previously depicted in Figure 7.[8] Also, an incident particle's energy calculated from the measured gyroradius can be validated with neutral beam energy measurements since these particles, by definition of being prompt losses, undergo minimal interactions with other plasma species and are lost from the system before substantial energy transferring collisions can occur. After determining which neutral beam injector incident fast ions of interest originated from, the code allows a neutral beam footprint to be drawn behind the calculated reverse-orbits, providing an indication of the

likely locations and times of origin of detected fast ions. Thus, if the reverse orbit calculation code generates the same prompt loss transit times as experimentally measured transit times using inputs provided by the strike maps of interest to validate, then these generated strike maps are quantitatively accurate. Due to the different geometries and locations of the FIELD detectors on DIII-D, as depicted in Figure 2,[10] two mesh generation routines must be validated using this methodology to ensure both detectors' strike maps provide accurate measurements of incident ions' gyroradii and pitch angles. This diagnostic is an important tool for other studies require fast ion loss detectors to determine the characteristics of fast ions being ejected by other transport mechanisms, and thus the validation of the strike map generation code will be a beneficial contribution to this area of research.[2,9]

# Results

## Summary

The objective of this study was to address the accuracy of generated strike maps that overlay optical FILD scintillator signals, as depicted in Figure 7.[8] Neutral beam current signals with finer time resolution provided a more precise measurement of the onset of neutral beam injection into DIII-D when compared to the FIDA signal used previously. A reverse orbit calculation code, which requires information provided by the calculated strike maps for particular prompt losses of interest, was used to simulate prompt loss trajectories and calculate likely fast ion transit times. Conformity between measured and simulated transit times would indicate the generated strike maps are quantitatively accurate.

Various shots were analyzed from June 30, 2011 and August 16, 2011 that yielded repeated prompt-loss signals. Due to the characteristic time scales of prompt losses of dozens of microseconds, and the in phase nature of these losses with respective neutral beam signals, it was possible to differentiate prompt losses from other instability driven losses. A neutral beam current signal with a typical FILD PMT signal indicating observed losses were most likely prompt losses are depicted in Figure 12. Measured transit times ranged from 10 microseconds to 90 microseconds, which were the expected transit times for prompt losses while considering typical neoclassical orbits path lengths and fast ion velocities. Simulation transit times using inputs from calculated strike maps overlaying optical FILD signals were consistent with measured results to within experimental uncertainties. Specific results are presented as representative of the various shots analyzed to determine the accuracy of strike maps for both FILD detectors.



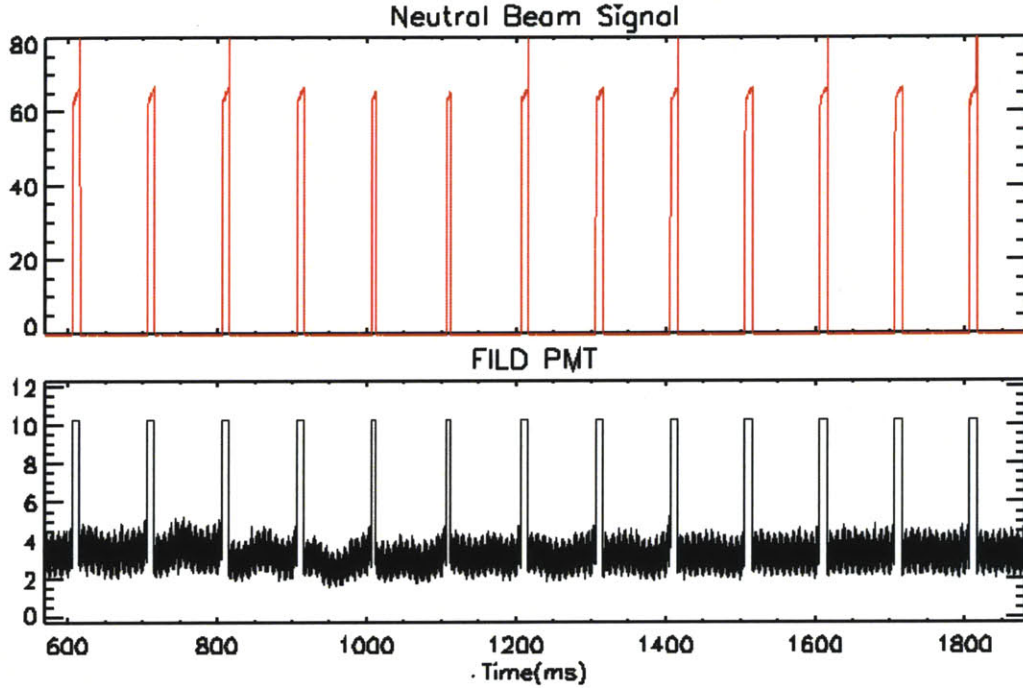


Figure 12. A typical neutral beam current signal with the resulting FILD PMT signal. The in phase, repeated waveforms of both signals along with nearly zero time offset between the signals indicate prompt-losses resulting from neutral beam injection. Furthermore, the slightly shorter neutral beam pulses in the time interval from 1000 to 1200 ms is reflected in the slightly shorter FILD PMT square wave width, suggesting these prompt losses are certainly due to neutral beam injection.

### FILD1 Results

One particular shot of interest yielded prompt loss signals at the FILD1 detector resulting from  $210^0$  neutral beam injection during the plasma current ramp up. The experimentally measured transit time between the onset of the neutral beam current signal and FILD PMT detection was  $90 \pm 10 \mu s$ . This ninety microsecond interval was presented in Figure 10 as a representation of the finer resolution neutral beam signals. A strike map was generated, and the resulting pitch angles and full neutral beam energy of incident ions were used as inputs to the reverse orbit calculation code. The simulation transit time results indicated possible transit times ranging from  $82.4$  to  $87.8 \mu s$ , which is consistent with experimental transit times to within experimental uncertainties. The simulation results are depicted in Figure 13. Though the reverse orbit trajectory crosses the neutral beam location four times, only two overlaps were consistent with an initial fast ion velocity counter the plasma current,

as required from the countercurrently injecting  $210^0$  neutral beam.

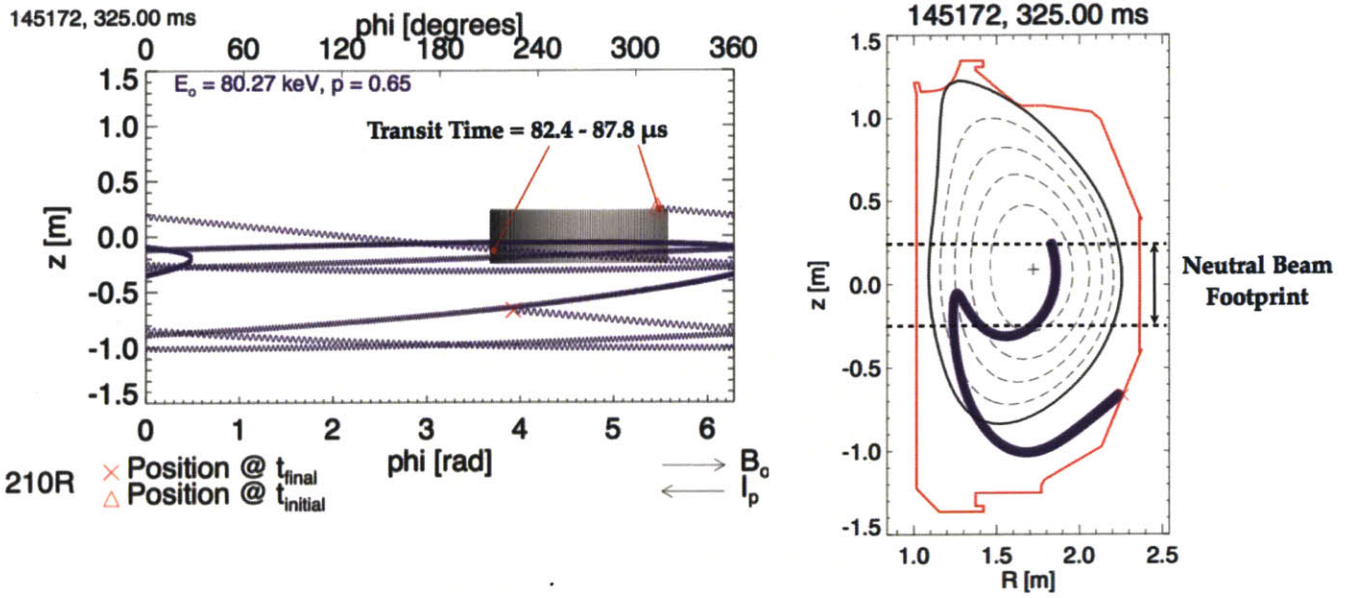


Figure 13. Simulation transit times for representative shot 145172 at 325 ms. The range of transit times at the extrema of the intersections with the  $210^0$  neutral beam footprint are depicted. Note the initial velocity at each extrema point is counter the plasma current, consistent with the  $210^0$  neutral beam injecting countercurrently. The same orbit is plotted in a poloidal cross section on the right, showing the neoclassical orbit detected ions likely underwent while traveling to the FILD1 detector located below the mid-plane of the torus. Note that the initial and final locations on the left, toroidal plot refer to likely points of ionization and FILD detector location, respectively.

## FILD2 Results

The FILD2 PMT signal resulting from the neutral beam injection, previously depicted in Figure 12, is used here at 1205 ms as a representative FILD2 result used to determine the accuracy of FILD2 strike maps. This specific prompt loss event of interest yielded an experimental transit time of  $17 \pm 10 \mu s$  of fast ions resulting from  $210^0$  neutral beam injection. This transit time is notably shorter than the experimental time used in the representative FILD1 signal in the previous section, primarily due to the different FILD2 location near the midplane, larger plasma current during the FILD2 prompt loss signal, and a substantially different plasma shape. Strike maps were generated as depicted in Figure 7, and the resulting pitch angles and energies were used as inputs to the reverse orbit calculation. The results of the reverse orbit calculation are depicted in Figure 14, resulting in a transit time of



12.57 $\mu$ s. A secondary overlap of the reverse orbit trajectory and neutral beam footprint was not observed as in the FILD1 representative reverse-orbit calculation since the reverse orbit trajectory intersected the wall before a secondary crossing could occur. Thus, this confirms the observed prompt losses shown in Figure 14 must have been born during the single pass through the neutral beam footprint, with a maximum transit time of 12.57 $\mu$ s. Given the ten microsecond uncertainty in experimental transit times, the simulation and experimental transit times for this representative prompt loss event were consistent.

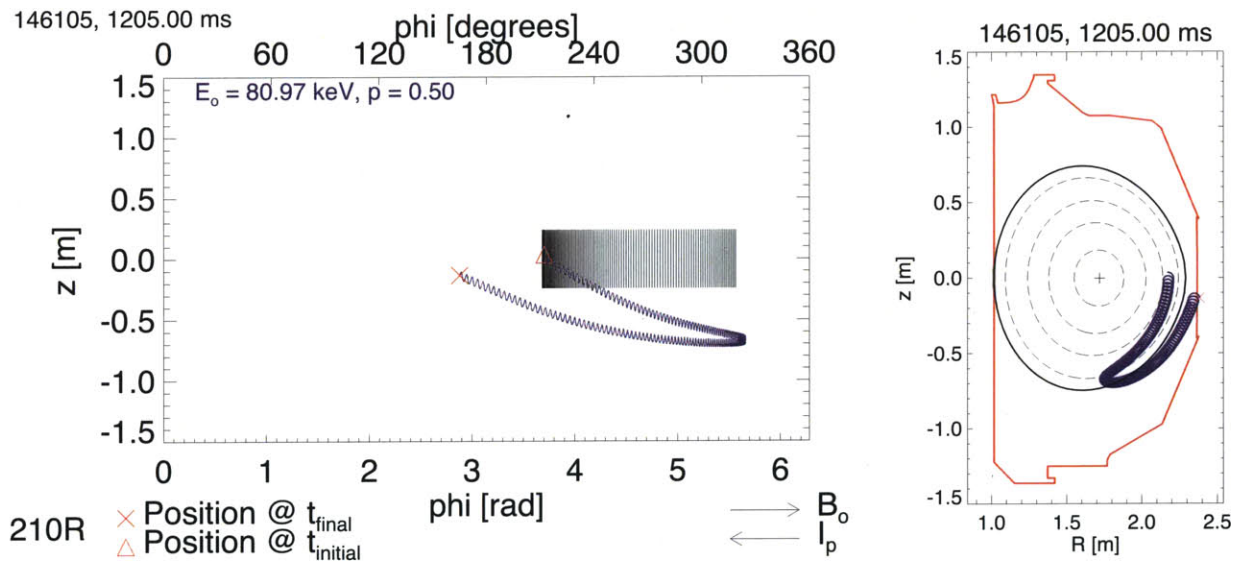


Figure 14. Simulation transit times for representative shot 146105 at 1205 ms. The reverse time trajectory of fast ions only crossed the 210<sup>0</sup> neutral beam footprint once before intersecting the wall, terminating the reverse orbit calculation. Note the initial velocity is counter the plasma current direction, which is expected for the 210<sup>0</sup> neutral beam that injects countercurrently. Note that the initial and final locations on the left, toroidal plot refer to likely points of ionization and FILD detector location, respectively.

# Discussion and Conclusion

The objective of this study was to validate the accuracy of generated strike maps that overlay optical FILD signals and yield incident ions' gyroradii and pitch angles. Multiple prompt loss signals were observed by both FILD detectors over a series of shots with a variety of plasma conditions, such as varying plasma currents and plasma shaping, which have the most substantial effect on promptly lost fast ion transit times. Consistency between experimental transit times and reverse orbit transit times to within experimental uncertainties conditions was observed repeatedly, indicating the generated strike maps for both FILD detectors are accurate. The neutral beam current signals used in this study provided a nearly three fold improvement in time resolution compared to the FIDA signals used previously to indicate the onset of neutral beam injection into DIII-D, depicted in Figure 9.[3] This neutral beam signal with ten microsecond time resolution allowed a more accurate determination of fast ion transit times than was previously possible. Thus, through the methodology presented, these new neutral beam signals enabled the accuracy of strike maps to be determined more precisely, and were found to be accurate to within experimental uncertainties.

Though better experimental time resolution has enabled a more substantial validation of the accuracy of generated strike maps, this analysis was limited by spatial scintillator resolution in both FILD detectors. This limitation is more pronounced in the FILD2 detector since it encompasses a smaller solid angle of scintillation material in view of the CCD camera when compared to FILD1. When analyzing both FILD detectors, the pitch angles of incident ions could only be determined to within  $5^\circ$  accuracy, which translates into an uncertainty in simulated reverse orbit transit times that require the input of pitch angle to calculate the reverse orbits. Though incident ions' gyroradii are also subject to this limitation in spatial resolution, this study focused on prompt losses which by definition are lost from the system before any interactions with other plasma species can occur. Therefore, the incident ion energy is equal to the full neutral beam energy, or predictable fractions of

the full neutral beam energy for different molecular configurations of energetic deuterium neutrals. The variation in simulation times resulting from a  $10^0$  total variation in pitch angle around a particular value differs depending on plasma conditions and the location of the FILD detector.

An analysis of the sensitivity of reverse orbit trajectories to variations in pitch angles was conducted on prompt loss signals from both FILD detectors. It was found that  $5^0$  errors in pitch angle can lead to upwards of twenty microsecond uncertainties in reverse-orbit transit times calculated from FILD1 detector results whereas only five microsecond uncertainties in reverse orbits from the FILD2 detector. Thus, the FILD2 reverse-orbit calculations seem to be more robust to pitch angle errors when compared to FILD1 calculations. Fortunately, the FILD1 detector has better spatial resolution than the FILD2 detector simply from detector geometry considerations, which on average leads to smaller uncertainties in pitch angle in the FILD1 detector. A more expansive analysis of the sensitivity of reverse orbit calculated transit times to variations in pitch angle should be conducted in future work to determine if an investment in higher resolution cameras would be beneficial, or if this pitch angle uncertainty is inevitable due to the material limitations of the scintillator.

# Extensions

The validation of the accuracy of strike maps is beneficial to other studies that will use FILD system on DIII-D, including current fast ion transport studies that hope to expand the understanding of fast ion transport by Alfvén eigenmodes.[2,9] In future, predominately self-heated DT fusion reactors such as ITER, 3.5 MeV fusion born alpha particles, and other highly energetic particles driven by external heating systems, will be the primary sources of energy to maintain thermonuclear temperatures. The 3.5 MeV alpha particles will be supersonic relative to the Alfvén velocities in ITER, creating shockwaves that could induce and amplify toroidal Alfvén eigenmodes (TAEs), otherwise known as gap modes. This interaction could have a destabilizing effect on the fusion system such to increase the magnitude of TAE instability due to the weaker damping term governing the evolution of TAEs when compared to the more strongly damped shear Alfvén waves.[11] This amplified TAE instability could result in increased fast ion transport, which could jeopardize the fusion power balance and damage first wall materials that are inundated with ejected fast ions. TAEs were first confirmed experimentally in the Tokamak Fusion Test Reactor (TFTR) when neutral beam injection was used to provide the fast ions in the system, and would only be amplified further in a self-heated reactor scenario such as ITER which will rely on a large population of alpha particles for power balance.[11] Thus, it is imperative to better understand the extent of fast-ion transport by fast-ion induced TAEs and achieve proper mitigation to ensure the success of future self-heated fusion reactors such as ITER. One critical diagnostic for studying fast ion transport by TAEs is the FILD detector, and the validation of the accuracy of strike maps will be beneficial to ensure the accuracy of data acquired from this diagnostic.

## REFERENCES

- [1] EESTER, D.V.: *ITER and Fusion Energy*. <http://iter.rma.ac.be/en/physics/tokamak/index.php>.  
Version: April 2012
- [2] FISHER, R.K. ; BOIVIN, R. ; FREDERICKSON, E. ; GARCIA-MUNOZ, M. ; HEIDBRINK, W.W. ; MUSCATELLO, C. ; NAZIKIAN, R. ; PACE, D.C. ; PETTY, C.C. ; ZHU, M.A. Van Z.: Measurements of Beam Ion Losses on DIII-D Due to MHD Instabilities. Dublin, Ireland, June 2010
- [3] FISHER, R.K. ; PACE, D.C. ; GARCIA-MUNOZ, M. ; HEIDBRINK, W.W. ; MUSCATELLO, C.M.: Scintillator-based diagnostic for fast ion loss measurements on DIII-D. In: *Rev. Sci. Instrum.* 81 (2010), Nr. 10D307
- [4] FRIEDBERG, Jeffery P.: *Plasma Physics and Fusion Energy*. Cambridge University Press, 2007
- [5] GARCIA-MUNOZ, M. ; PACE, D.C. ; FISHER, R.K. ; ZEELAND, M. V.: *FILD at DIII-D*. DIII-D Physics Meeting, January 2010
- [6] HARTWIG, Zachary S. ; PODPALY, Yuri A.: *Magnetic Fusion Energy Formulary*. Massachusetts Institute of Technology, November 2011
- [7] HEIDBRINK, Bill ; MUSCATELLO, Chris: *The DIII-D Fast-Ion Deuterium-Alpha (FIDA) Diagnostic*. <https://diii-d.gat.com/diii-d/FIDA>. Version: April 2012
- [8] PACE, D.C.: *FILD2 Mapping Presentation*. DIII-D Physics Meeting, May 2011
- [9] PACE, D.C. ; FISHER, R.K. ; GARCIA-MUNOZ, M. ; HEIDBRINK, W.W. ; MCKEE, G.R. ; MURAKAMI, M. ; MUSCATELLO, C.M. ; NAZIKIAN, R. ; PARK, J.M. ; PETTY, C.C. ; RHODES, T.L. ; STAEBLER, G.M. ; ZEELAND, M.A. V. ; WALTZ, R.E. ; WHITE, R.B. ; YU, J.H. ; ZHANG, W. ; ZHU, Y.B.: Transport of energetic ion due to sawteeth, Alfven eigenmodes, and microturbulence. In: *Nuclear Fusion* 51 (2011), April, S. 8
- [10] PACE, D.C. ; FISHER, R.K. ; GARCIA-MUNOZ, M. ; HEIDBRINK, W.W. ; ZEELAND, M.A. V.: Convective beam ion losses due to Alfven eigenmodes in DIII-D reversed-shear plasmas. In: *Plasma Physics and Controlled Fusion* 53 (2011)
- [11] WESSON, John: *Tokamaks*. Fourth Edition. Oxford University Press, Oxford Science Publications, 2011 (International Series of Monographs on Physics - 149)